ARMY RESEARCH LABORATORY

Refractive Index Measurement of Fibers Through Fizeau Interferometry

by Brian E. Parquette and Daniel J. O'Brien

ARL-TR-6548 August 2013

NOTICES

Disclaimers

The findings in this report are not to be construed as an official Department of the Army position unless so designated by other authorized documents.

Citation of manufacturer's or trade names does not constitute an official endorsement or approval of the use thereof.

Destroy this report when it is no longer needed. Do not return it to the originator.

Army Research Laboratory
Aberdeen Proving Ground, MD 21005-5066

ARL-TR-6548 **August 2013**

Refractive Index Measurement of Fibers Through Fizeau Interferometry

Brian E. Parquette and Daniel J. O'Brien
Weapons and Materials Research Directorate, ARL

REPORT DOCUMENTATION PAGE	Form Approved OMB No. 0704-0188

1. REPORT DATE *(DD-MM-YYYY)*	2. REPORT TYPE	3. DATES COVERED (From - To)
August 2013	Final	1 November 2011–30 May 2013

4. TITLE AND SUBTITLE
Refractive Index Measurement of Fibers Through Fizeau Interferometry

5a. CONTRACT NUMBER

5b. GRANT NUMBER

5c. PROGRAM ELEMENT NUMBER

6. AUTHOR(S)
Brian Parquette and Daniel J. O'Brien

5d. PROJECT NUMBER

5e. TASK NUMBER

5f. WORK UNIT NUMBER

7. PERFORMING ORGANIZATION NAME(S) AND ADDRESS(ES)
U.S. Army Research Laboratory
ATTN: RDRL-WMM-A
Aberdeen Proving Ground, MD 21005-5066

8. PERFORMING ORGANIZATION REPORT NUMBER
ARL-TR-6548

9. SPONSORING/MONITORING AGENCY NAME(S) AND ADDRESS(ES)

10. SPONSOR/MONITOR'S ACRONYM(S)

11. SPONSOR/MONITOR'S REPORT NUMBER(S)

12. DISTRIBUTION/AVAILABILITY STATEMENT
Approved for public release; distribution is unlimited.

13. SUPPLEMENTARY NOTES

14. ABSTRACT
The optical properties of transparent polymer fibers are investigated for use in transparent composite materials using a Fizeau interferometer. Refractive index and thermo-optic measurements are performed for off-the-shelf and internally manufactured fibers. The interferometer is shown to produce accurate, repeatable results for fibers with a cross-sectional area of over 500 μm2. Results show that manufacturing variables can have significant effects on the optical properties of polymer fibers, particularly birefringence.

15. SUBJECT TERMS
composite, transparent, refractive index, refractometry, interferometer

16. SECURITY CLASSIFICATION OF:			17. LIMITATION OF ABSTRACT	18. NUMBER OF PAGES	19a. NAME OF RESPONSIBLE PERSON
a. REPORT	b. ABSTRACT	c. THIS PAGE			Brian E. Parquette
Unclassified	Unclassified	Unclassified	UL	24	19b. TELEPHONE NUMBER (*Include area code*) (410) 306-2571

Standard Form 298 (Rev. 8/98)
Prescribed by ANSI Std. Z39.18

Contents

List of Figures

List of Tables

INTENTIONALLY LEFT BLANK.

1. Introduction

Over time, fiber-reinforced composites have developed as an increasingly attractive alternative to traditional monolithic materials. Their unique mechanical properties and adaptability offer many advantages over more conventional materials. Recent work has suggested that it may be possible to adapt fiber-reinforced composites to transparent armor applications (*1*). However, these transparent composites require fibers with very specific and highly calibrated optical properties, particularly refractive index.

Refractive index measurement of transparent fibers has long presented a significant challenge. Abbe refractometry, the typical measurement technique for bulk materials and liquids, requires a sizeable flat surface to achieve optical contact with a prism, thus it is unfeasible for measuring a thin fiber (*2*). Previous work has demonstrated refractive index measurement of fibers through submersion in fluid of a known index (*1*), but this method is time consuming, and does not deliver the high degree of accuracy or flexibility necessary for the present application. Other techniques, such as the Becke line method (*3*) and the Christiansen-Shelyubskii method (*4*), have been used to characterize fibers but do not grant the necessary precision.

An alternative method for measuring a fiber's refractive index involves the measurement of Fizeau fringes produced by multiple-beam interferometry (*5*). Here we adapt this method for efficient measurement of the refractive index of varied fiber materials and sizes across the visible spectrum. A Fizeau interferometer is constructed from off-the-shelf parts. Additionally, the technique is modified to enable measurement of the refractive index's temperature dependence (dn/dT). Measured values of each property are compared with published values and previous work to evaluate the level of accuracy and consistency in the system. Variables in fiber processing and material are appraised for their respective effects on relevant optical properties and suitability for composite applications.

2. Fizeau Interferometry

Fiber refractive index is characterized in this work via Fizeau interferomtery. In this technique, monochromatic light is collimated and directed into a silvered wedge, as shown in figure 1. The wedge is filled with fluid of a known refractive index, and a fiber is immersed in the fluid with its axis perpendicular to the apex of the wedge. In the transmitted light, the partially reflective surfaces create a series of interference fringes parallel to the apex of the wedge. As the fringes cross the fiber they are shifted by an amount dependent on the difference between the fiber index and the fluid index.

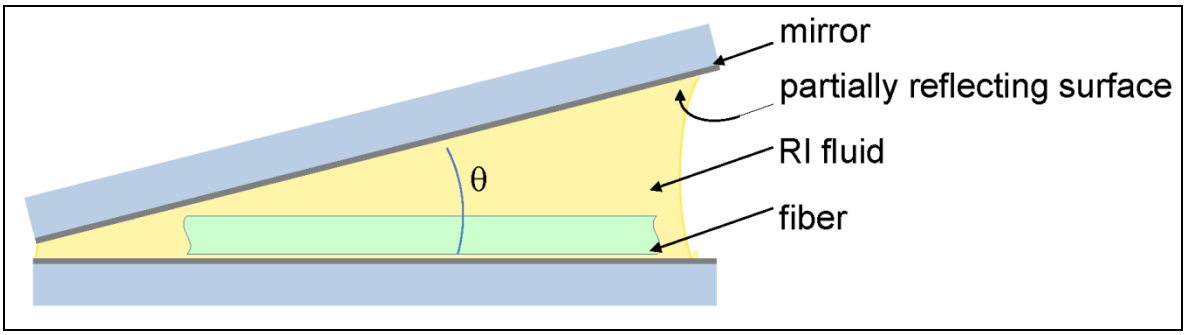

Figure 1. Diagram of interferometer wedge for fiber measurement.

The interferometer used in this work was constructed from off-the-shelf parts listed in table 1, which gives the manufacturer and part number of each component. A variety of low-power lasers (table 2) were used as light sources for measuring the refractive index across a range of wavelength. Figure 2 shows the interferometer setup consisting of a laser light source, converging lens, aperture, collimating lens, polarizer, mirror, two partially reflecting mirrors to form the wedge, a charge-coupled device (CCD) camera for imaging, as well as an assortment of optical fixtures for mounting the components.

For measuring how refractive index of the fiber changes with temperature (dn/dT), thin strip heaters were placed around the interferometer wedge and heated to a set temperature (figure 3). A thermocouple (CHAL-0005, Omega Engineering Inc., Stamford, CT) was placed inside the wedge to measure the internal temperature, while an additional thermocouple was placed outside the wedge to measure and control the temperature of the heaters.

Table 1. Interferometer components.

Component	Manufacturer	Part Number
Converging lens	Carl Zeiss AG (Oberkochen, Germany)	Plan-Neofluar 10x/0.3 440330
Aperture	Edmund Optics, Inc. (Barrington, NJ)	NT53-915
Collimating lens	CVI Melles Griot (Albuquerque, NM)	LPX-75.0-96.0-C-SLMF-400-700
Polarizer	CVI Melles Griot	FPG-50.8-5.3
Mirror	CVI Melles Griot	PAV-MPG-5010M-LEBG
Optical flats	CVI Melles Griot	PR1-589-70-2037
CCD camera	Lumenera Corp. (Ottawa, Canada)	Infinity3-1
Strip heaters	McMaster-Carr (Chicago, IL)	35475K722
Temperature controller	Glas-Col, LLC (Terre-Haute, IN)	DigiTrol II

Table 2. Lasers used in interferometer for fiber refractive index measurement.

Manufacturer	Model	Wavelength
Laserglow Technologies, Inc. (Toronto, Canada)	Blue Aquarius-5	473 nm
Thorlabs (Newton, NJ)	CPS532	532 nm
Laserglow Technologies, Inc.	Yellow Rigel HV-5	589 nm
Thorlabs	CPS182	635 nm
Thorlabs	CPS184	650 nm
Thorlabs	CPS186	670 nm

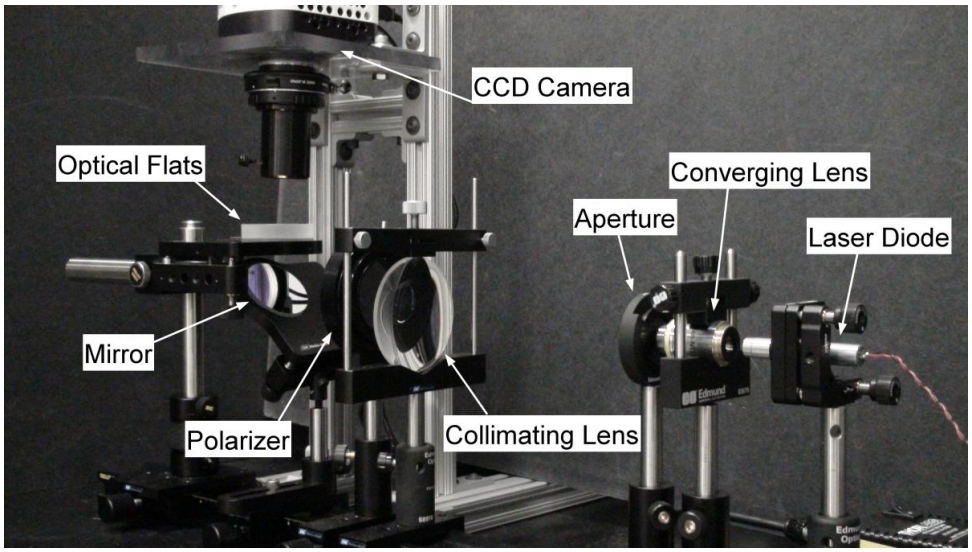

Figure 2. Setup and components of the interferometer.

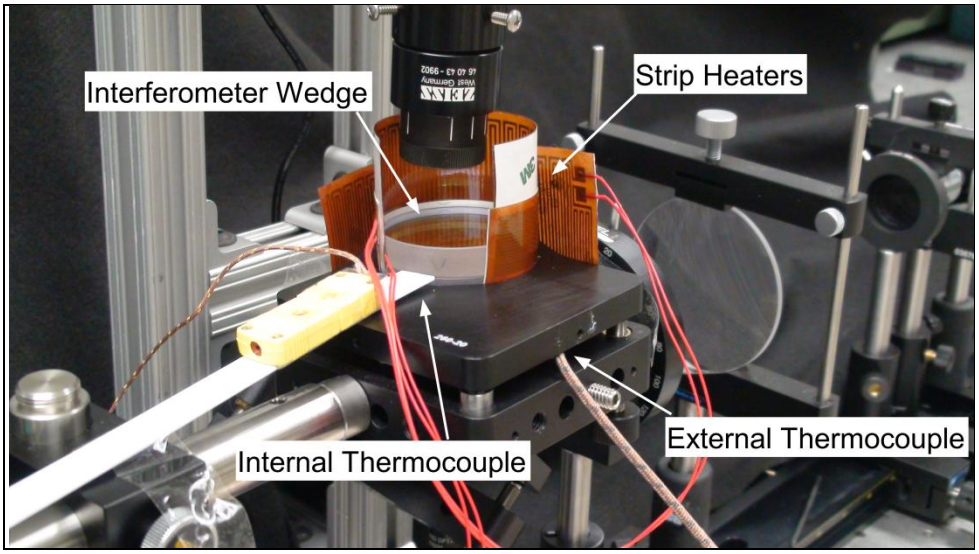

Figure 3. Setup of the interferometer for dn/dT measurement.

3. Experimental Procedure

3.1 Materials

The fluids used in the interferometer wedge were combinations of 1.459 and 1.570 index liquids (5040 Immersion Liquid, Cargille Labs, Cedar Grove, NJ) mixed in specified amounts to produce the desired refractive index. After mixing, the fluid's index was measured across the visible spectrum using an Abbe refractometer (DR-M2, Atago Co., Ltd., Tokyo, Japan). The refractometer was illuminated by a white light source coupled with monochromatic filters of various wavelengths. Heated water of various temperatures was pumped through the refractometer to measure the dn/dT of the fluid.

The set of fibers tested included three externally manufactured fibers: Pro Line 4-lb, 200-μm Premium natural clear nylon monofilament (Cabela's, Sidney, NE), 449-AA-250 S-2 glass (AGY, Aiken, SC), and SMF28 single-mode optical fiber (Corning Inc., Corning, NY), along with a variety of internally manufactured polypropylene (PP) and Trogamid* nylon fibers. The Pro Line was a round fiber as-received but was flattened by a continuous pull method through a pair of 25.4-mm-diameter hardened steel nip rollers (*1*). Related work describes the processing and characterization of the PP and nylon fibers in greater depth (*6*).

3.2 Procedure

Following alignment of the optical components, the fiber specimen was placed on the lower optical flat and oriented perpendicular to the apex of the wedge. Spacers were placed alongside the fiber to achieve a sufficient gap thickness to accommodate the fiber, as well as to create a wedge angle of 5×10^{-3} to 1×10^{-4} radians (*5*). A fluid of a known refractive index was then added and the top optical flat was placed on the spacers, forming a wedge of liquid between the two flats (figure 2). A laser of a given wavelength was directed into the apparatus, illuminating the fiber inside the wedge, and the polarizer was adjusted to align the light to be polarized either parallel or perpendicular to the fiber axis. A CCD camera was used to take images of the Fizeau fringes formed in the wedge at the point where they crossed the fiber (figure 4).

*Trogamid is a registered trademark of Evonik Industries, AG, Essen, Germany.

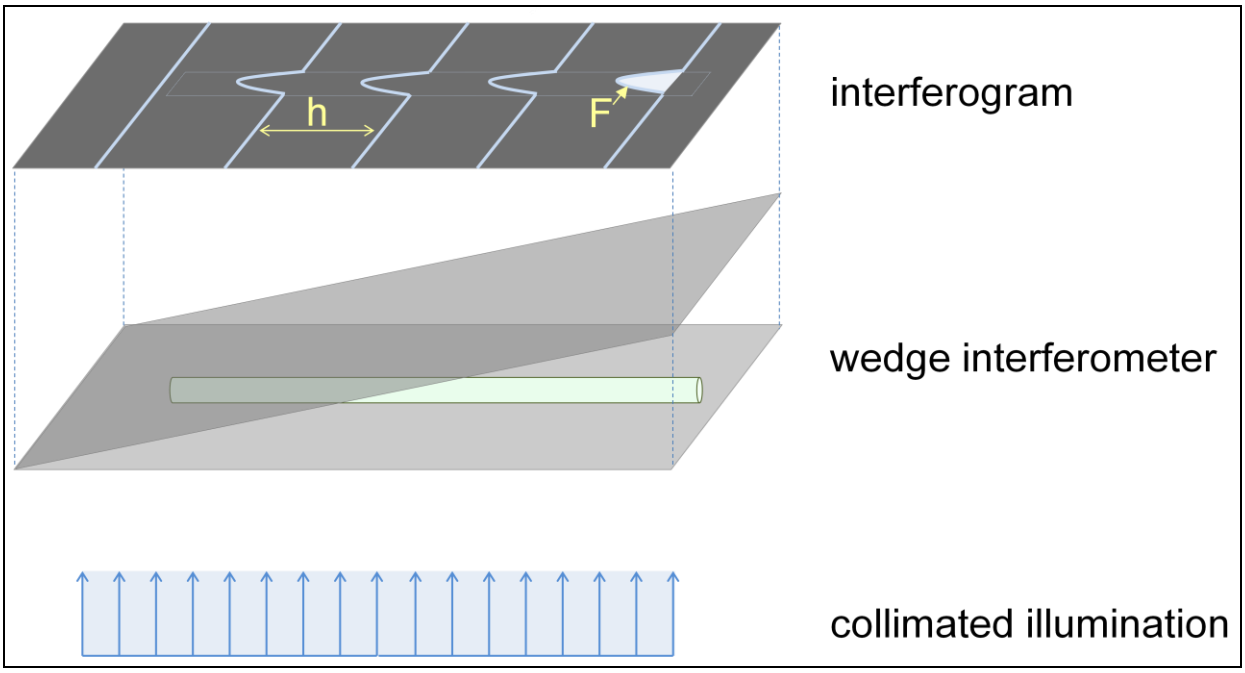

Figure 4. Diagram of fiber interferogram acquisition.

From the images produced in this process, the refractive index of the fiber was calculated by

$$n_F = n_L + \frac{F\lambda}{2hA},$$

where n_F is the fiber index, n_L is the liquid index, F is the fringe shift area, λ is the laser wavelength, h is the interfringe spacing, and A is the fiber cross-sectional area. If the fringe shift is toward the apex of the wedge, F will be positive; if the shift is away from the apex, F will be negative.

Most fibers were measured a single time at each wavelength, although many of the 473-nm images were discarded due to the low image quality produced with this laser. In a few cases, the fibers were measured only at a single wavelength either due to measurement difficulties or because just a single test was needed to compare with past measurements. A selection of the fibers were measured 2–3 times at one or all wavelengths to establish the repeatability of the measurement. In these cases, a new length of fiber from the same spool was used for each successive test.

For dn/dT testing, the interferometer was modified as described previously, and the attached heaters were set to the desired temperature. After a stable internal temperature had been established for at least 30 min, an image of the fringes was taken as previously discussed. All dn/dT testing was performed using the 532-nm laser.

4. Results

4.1 Refractive Index Measurements

Table 3 shows the measured refractive indices for fibers measured in the interferometer. All listed measurements were conducted at room temperature. The refractive index in the direction parallel to the fiber axis is represented by ($n^{\parallel}$), while the index perpendicular to the fiber axis is represented by ($n^{\perp}$).

Table 3. Refractive index measurements of fibers for all wavelengths measured.

	473 nm	532 nm	589 nm	635 nm	650 nm	670 nm
S2 Glass	—	1.5263 ±0.0032	—	—	—	—
Optical Fiber Cladding	—	1.4621 ±0.0003	1.4579 ±0.0002	1.4551 ±0.0001	1.4544 ±0.0001	1.4535 ±0.0000
Flat Nylon Fishing Line ∥	—	1.5706 ±0.0012	1.5665 ±0.0017	1.5631 ±0.0028	1.5634 ±0.0018	1.5624 ±0.0016
Flat Nylon Fishing Line ⊥	—	1.5497 ±0.0033	1.5434 ±0.0032	1.5422 ±0.0036	1.5408 ±0.0023	1.5403 ±0.0023
PP Round ∥	—	—	1.5065	—	—	—
PP Round ⊥	—	—	1.4982	—	—	—
PP Multifilament #2 ∥	1.5171	1.5138 ±0.0053	1.5053	1.5048	1.5039	1.5029
PP Multifilament #2 ⊥	1.5064	1.4957 ±0.0034	1.4937	1.4917	1.4903	1.4900
PP Multifilament #7 ∥	1.5174	1.5162 ±0.0026	1.5070	1.5063	1.5058	1.5047
PP Multifilament #7 ⊥	1.4978	1.4951 ±0.0031	1.4913	1.4883	1.4900	1.4886
PP Monofilament Undrawn ∥	1.5123	1.5071	1.5030	1.5007	1.4998	1.4988
PP Monofilament Undrawn ⊥	1.5057	1.4976	1.4947	1.4888	1.4884	1.4878
PP Monofilament Drawn ∥	1.5128	1.5094	1.5048	1.5018	1.5009	1.5002
PP Monofilament Drawn ⊥	1.5058	1.4967	1.4930	1.4910	1.4906	1.4895
Nylon 2:1 ∥	—	1.5319	1.5284	1.5264	1.5259	1.5253
Nylon 2:1 ⊥	—	1.5176	1.5143	1.5123	1.5117	1.5112
Nylon 1.15:1 ∥	—	1.5190	1.5153	1.5128	1.5124	1.5118
Nylon 1.15:1 ⊥	—	1.5181	1.5144	1.5122	1.5117	1.5109

Figures 5 and 6 show typical interferograms for S2 glass and the optical fiber. These two fibers were of a known refractive index and were tested to confirm the accuracy of the interferometer. For these interferograms (and all that follow) the apex of the interferometer wedge is above the top edge of the image. This signifies that for fringes bending upward, as in the S2 glass, the refractive index of the fiber is higher than that of the surrounding liquid. Conversely, for fringes that bend downward, as in the optical fiber, the fiber has a lower refractive index than the fluid.

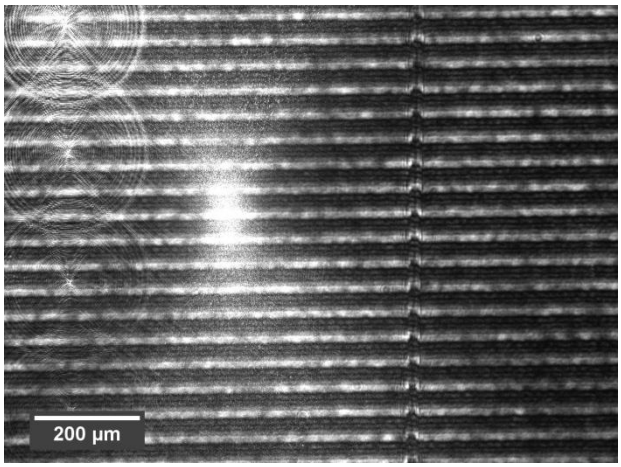

Figure 5. Interferogram of S2 glass in n = 1.5146 liquid with perpendicular polarized light at 589 nm.

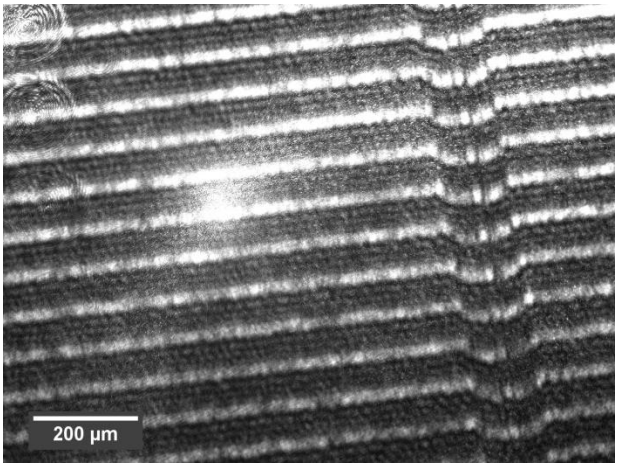

Figure 6. Interferogram of optical fiber in n = 1.4590 liquid with perpendicular polarized light at 650 nm.

These two interferograms also display the rounded fringe profile characteristic of fibers that have a round cross-section. Since the thickness of fiber that the light has to pass through is greater in the center of the round fiber than at the edge, the corresponding fringes are shifted to a greater extent in the center. As the thickness of the fiber approaches zero at its edge, the fringe shift similarly approaches zero.

The optical fiber is comprised of an 8-μm-diameter core surrounded by a cladding with a total diameter of 125 μm. In the interferogram, the core is visible as a slight discontinuity in the fringe pattern in the center of the fiber area. Since the small size of the core made it unfeasible to measure, only the cladding index was considered in this work.

Figures 7 and 8 show interferograms for the Pro Line fiber in both as-received and flattened states. The as-received fiber displays a typical fringe pattern for a round fiber. However, when flattened, the expected flat fringe profile is not produced. Instead the fringes become somewhat chaotic, rising and falling multiple times across the fiber width. This suggests strong nonuniformity of geometry and/or refractive index.

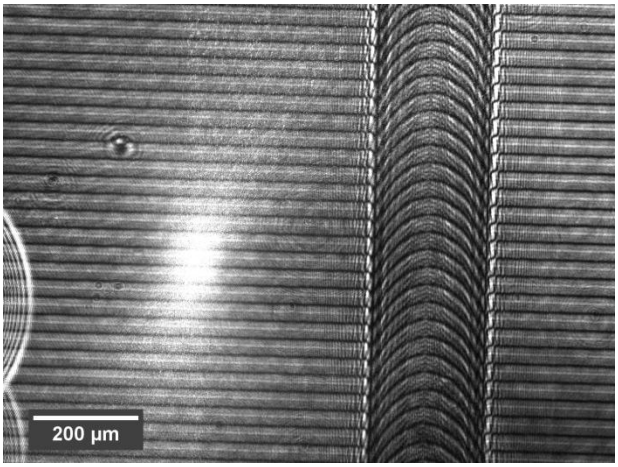

Figure 7. Interferogram of round nylon fishing line in n = 1.5111 liquid with perpendicular polarized light at 532 nm.

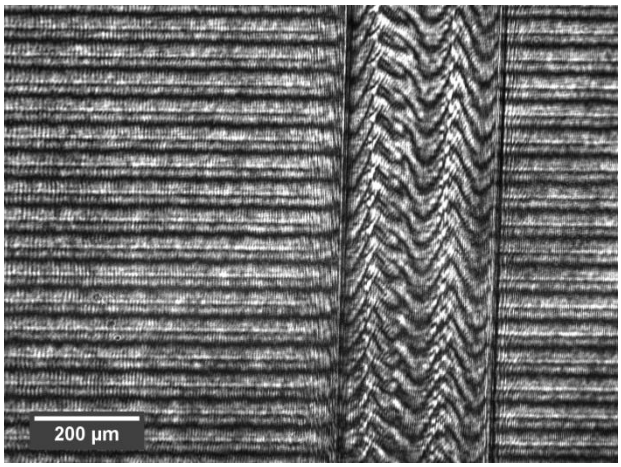

Figure 8. Interferogram of flat nylon fishing line in n = 1.5470 liquid with perpendicular polarized light at 635 nm.

Figure 9 shows typical interferograms for the PP multifilament for light polarized both parallel and perpendicular to the fiber axis. These images provide an example of a birefringent fiber and the effects of this birefringence. In the parallel orientation, the fringes bend upward toward the apex, signifying a refractive index higher than the 1.506 index of the liquid. In the perpendicular orientation, the same fiber produces fringes that bend downward, signifying an index below 1.506. Also of note in these interferograms is that the PP multifilament, being a flat, ribbon-shaped fiber, produces a flat fringe profile across most of the width of the fiber.

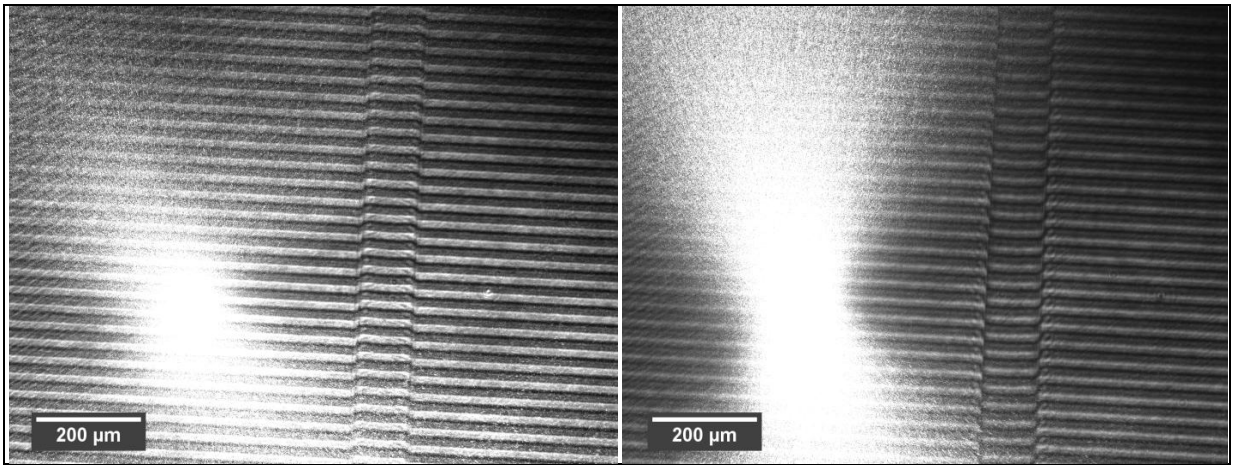

Figure 9. Interferogram of PP multifilament no. 2 in n = 1.5060 liquid with parallel (left) and perpendicular polarized light at 532 nm.

In figure 10 are interferograms of a similar PP multifilament, again showing strong birefringence. Although this is ostensibly a ribbon-shaped fiber, there is a degree of curvature in the fringes across the width of the fiber.

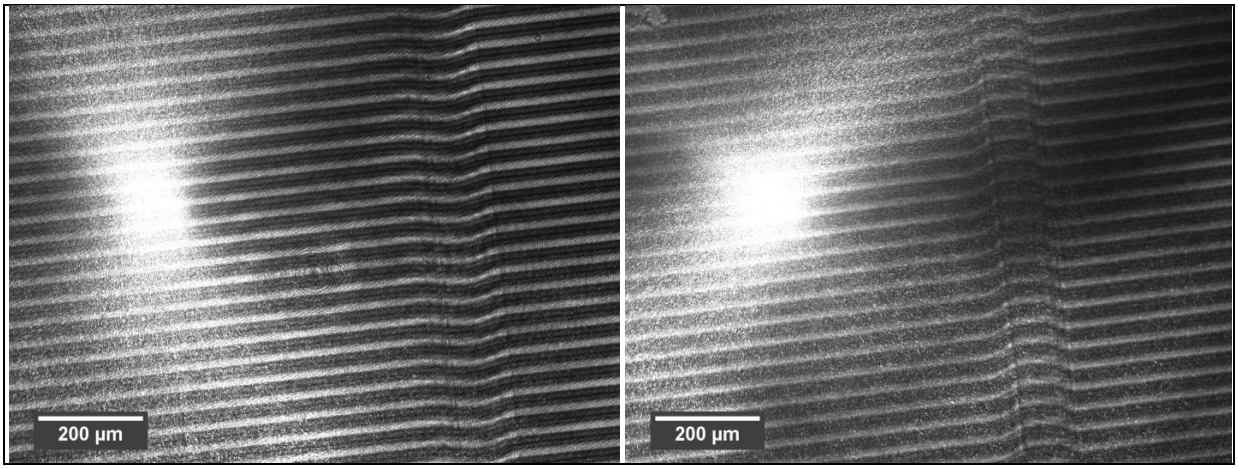

Figure 10. Interferogram of PP multifilament no. 7 in n = 1.4982 liquid with parallel (left) and perpendicular polarized light at 635 nm.

The PP monofilament (figure 11) was similar to the PP multifilament, with a larger cross-section and more ribbon-like profile. This fiber was examined in an undrawn state as well as with a 3.5:1 draw ratio. As can be seen in the interferograms, drawing produced a fiber with a much smaller width and with a slightly more rounded profile. Additionally, the refractive index was affected in both perpendicular and parallel polarizations, as can be seen in table 1.

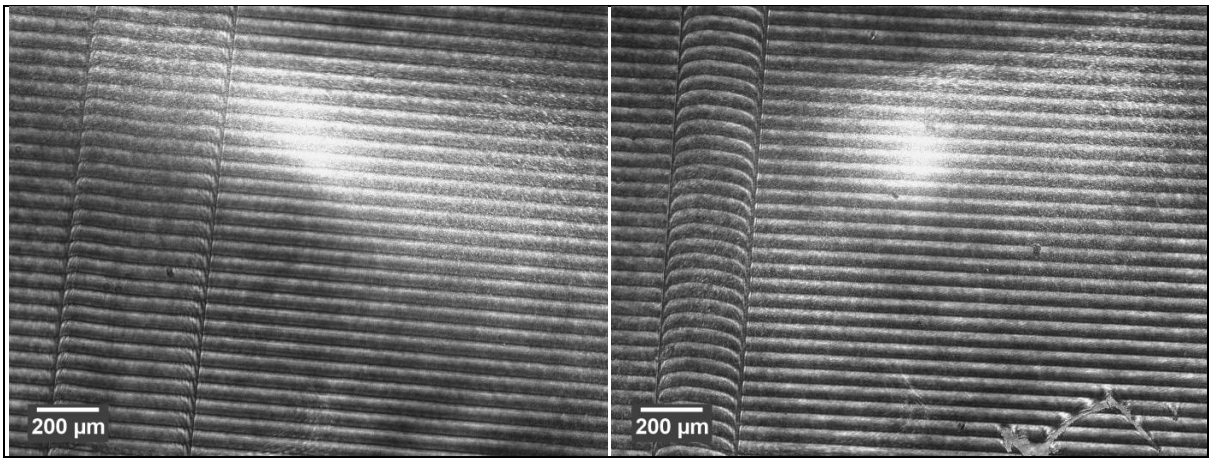

Figure 11. Interferogram of PP monofilament undrawn (left) and drawn (right) in n = 1.4982 liquid with parallel polarized light at 532 nm.

Figure 12 shows interferograms of a nylon ribbon fiber with a draw ratio of 1.15:1. The very low amount of anisotropy was immediately apparent when examining this fiber, with a difference between perpendicular ($n^{\perp}$) and parallel ($n^{\parallel}$) indices of just 0.0008 across the visible spectrum.

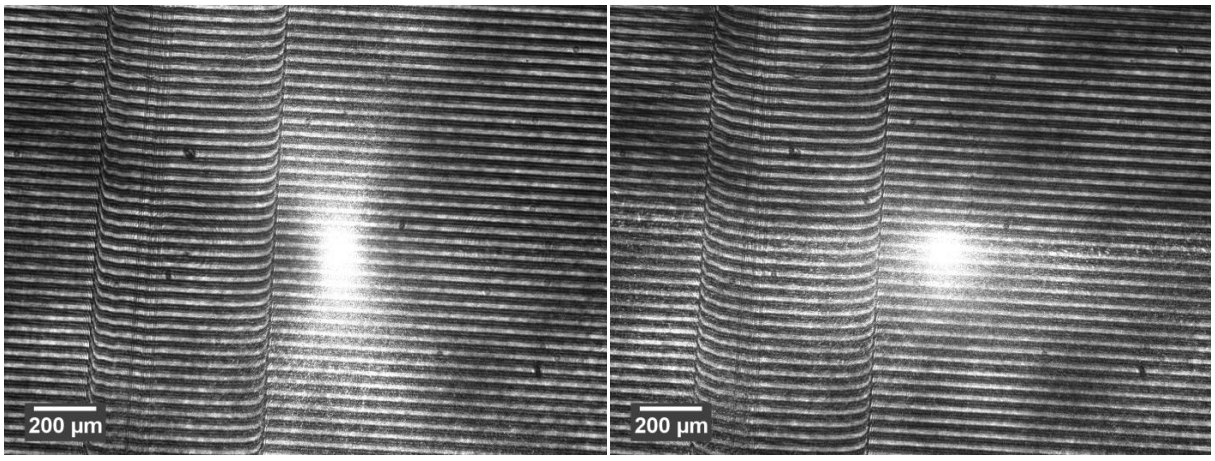

Figure 12. Interferogram of nylon 1.15:1 in, n = 1.5204 liquid with perpendicular (left) and parallel (right) polarized light at 532 nm.

4.2 Thermo-optic Measurements

Figure 13 shows dn/dT measurements at 532 nm for three different fibers: nylon 1.15:1, PP monofilament undrawn, and optical fiber. Both the nylon and PP monofilament are anisotropic fibers, so parallel and perpendicular indices are shown. The slope of the linear regression lines determines dn/dT, as shown in table 4.

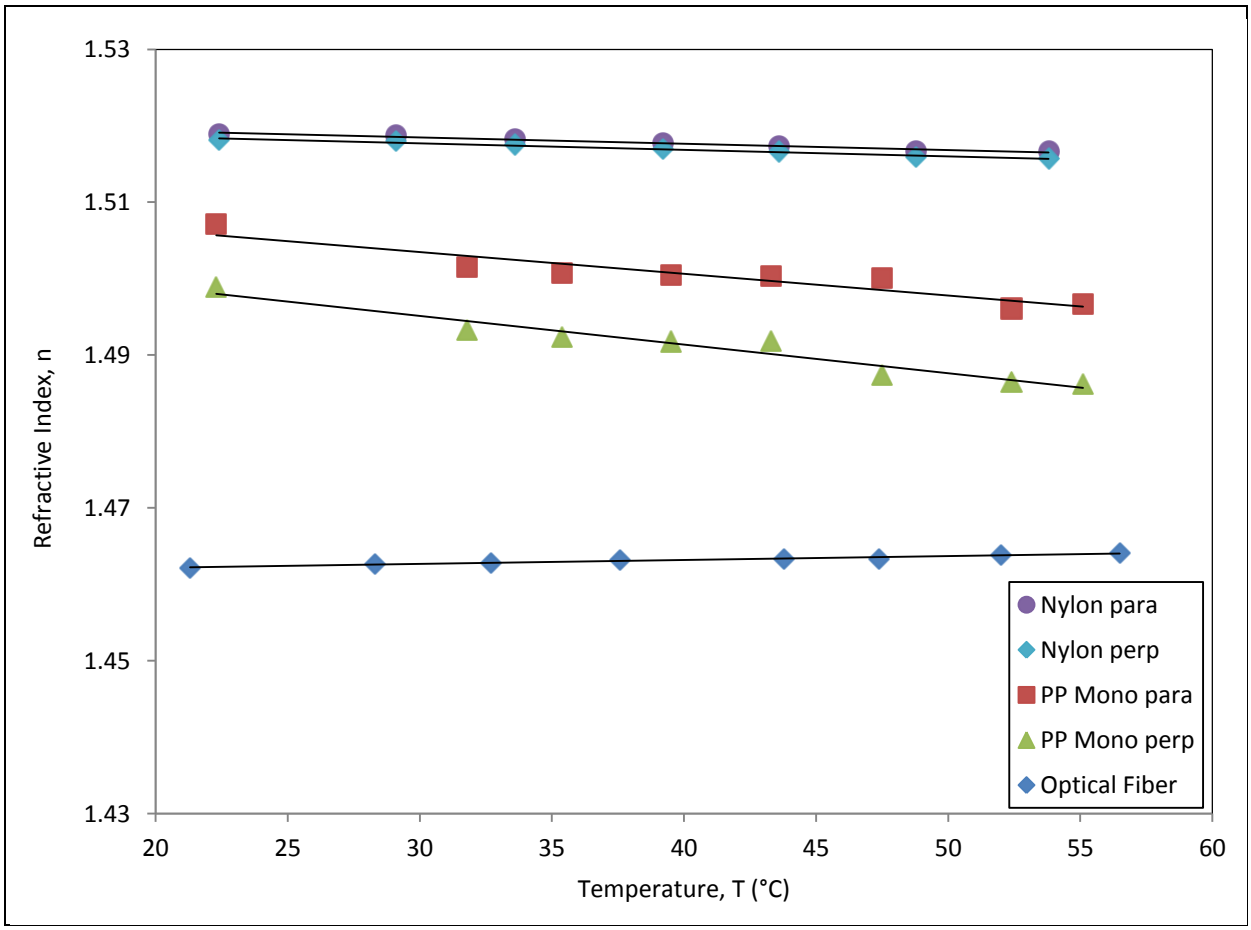

Figure 13. The dn/dT measurements at 532 nm for nylon 1.15:1, PP monofilament undrawn, and optical fiber.

Table 4. The dn/dT measurements at 532 nm.

Fiber	dn/dT ($°C^{-1}$)	Standard Deviation ($°C^{-1}$)
Nylon 1.15:1 ∥	-8.25×10^{-5}	5.36×10^{-6}
Nylon 1.15:1 ⊥	-8.59×10^{-5}	6.60×10^{-6}
PP mono undrawn ∥	-2.85×10^{-4}	4.40×10^{-5}
PP mono undrawn ⊥	-3.75×10^{-4}	3.78×10^{-5}
Optical fiber	5.06×10^{-5}	3.74×10^{-6}

5. Discussion

5.1 Refractive Index Measurements

To confirm the accuracy of this method of measurement, the measurements of fibers of known refractive index were compared with the values found in previous studies. The cladding of an optical fiber was known to be approximately 1.4597 (*7*) at a wavelength of 546 nm. Since no

measurement was made at this wavelength, a power-fit interpolation of the measured values to 546 nm was used reveal a refractive index of 1.4605, well within the acceptable range of error.

A similarly precise listed value for S-2 glass was not found, but the manufacturer lists the refractive index as 1.520–1.525 at 589.3 nm (*8*). A measured value of 1.5263 nm at 532 nm strongly predicts a 589-nm value within the listed range, and further measurements to confirm the accuracy were deemed unnecessary. The difficulty of measuring small-diameter fibers contributed to this reluctance to perform additional testing. The S2 fibers, at a cross-sectional area of just 330 μm², produced a much smaller fringe shift than larger fibers at comparative indices. The fringe shift is a function of the cross sectional area of the fiber, so the measurement resolution drops as fiber size decreases, and it becomes more difficult to acquire a precise measurement. All other fibers had a cross-sectional area of over 1000 μm², large enough to obtain refractive index values of a sufficient precision.

The PP round fiber was measured at 589 nm to compare with previous refractive index measurements made using the immersion technique. Through interferometry, the indices measured were $n^{\parallel} = 1.5065$ and $n^{\perp} = 1.4982$. Through immersion, the indices measured were $n^{\parallel} = 1.5070$ and $n^{\perp} = 1.4985$. With such a small difference in results produced, the two methods can be considered effectively identical in this application.

The flattened Pro Line proved difficult to measure due to the nonuniformity created during the rolling process. As seen in figure 7, the fringes were highly nonlinear across the fiber, likely due to a combination of inconsistencies in stress, density, and thickness. This nonuniformity would produce an inferior composite, with lower transparency and less consistent properties.

The internally manufactured fibers all proved to be more suitable. These fibers produced flat (figure 9) or rounded (figure 10) fringe profiles that were comparatively easy to measure and have been shown in other work to produce superior composite properties. Refractive index measurement at room temperature was performed across a range of wavelengths for a subset of the manufactured fibers.

The effects of drawing on these fibers are apparent from the PP monofilament interferograms (figure 11). As would be expected, the cross-section of the fiber decreased significantly, and the originally flat profile became slightly more rounded. More interestingly, the refractive index of the fiber was also altered. Drawing of the fiber is expected to produce a greater degree of alignment of the polymer chains along the fiber axis. In most cases, chain alignment in a polymer results in a greater degree of birefringence. At 532 nm, this was exactly the case, as $n^{\parallel}$ rose by 0.0023 upon drawing and $n^{\perp}$ dropped by 0.0008, changing the birefringence (Δn) of the fiber from 0.0096 to 0.0127.

The results become less clear at higher wavelengths. At 670 nm, $n^{\parallel}$ rose by 0.0013 and $n^{\perp}$ rose by 0.0017, dropping Δn from 0.0110 to 0.0107. The mechanics of this are unclear, and it may be that the absolute value of the change is so small in either case that it is falling within the standard

error of the measurement. This may in turn imply that the drawing process used for these fibers is not producing a significant change in the alignment of the polymer chains. Hamza et al. (*9*) made a similar measure of polypropylene at 546 nm and showed a Δn of approximately 0.0015 rising to 0.016 at corresponding draw ratios. This would suggest that the undrawn PP monofilament may already be in an aligned state equivalent to having been drawn, and drawing the fiber beyond this state produces little additional alignment.

For the nylon fibers, birefringence was clearly and significantly affected by the draw ratio. At a 2:1 draw ratio, the fiber produced fairly standard results, with a relatively consistent Δn of 0.015. At a 1.15:1 draw ratio, the birefringence was almost completely eliminated, with Δn below 0.001 for each wavelength measured. Both values are lower than that typically found for nylon 6 (*10*), although the change in birefringence upon drawing is in relatively good agreement. The discrepancy is likely due to nylon 6 being an imperfect match for the type of nylon used in manufacturing the fibers.

5.2 Thermo-optic Measurements

As with room temperature measurements, dn/dT measurements were initially evaluated using previously established values for the optical fiber cladding. As no known study existed specifically for optical-fiber cladding, values for fused silica were used instead. Fused silica was known to be the material used in the cladding for the SMF28 optical fiber. The measured value was determined to be 5.1×10^{-5} °C^{-1}, compared to the known value of 1.3×10^{-5} °C^{-1} (*11*). Although the measured dn/dT is higher than expected, the difference of 3.8×10^{-5} °C^{-1} was within the acceptable range of error. Also compared to the polymer fibers, the dn/dT of the optical fiber is much lower in magnitude and has positive sign, as expected.

The thermo-optic coefficient was also measured for representative samples of both the PP monofilament and nylon ribbon fibers. The undrawn PP monofilament produced results of $dn^{\parallel}/dT = -2.9 \times 10^{-4}$ °C^{-1} and $dn^{\perp}/dT = -3.8 \times 10^{-4}$ °C^{-1}. Previously published studies of undrawn polypropylene have found $dn^{\parallel}/dT = -3.9 \times 10^{-4}$ °C^{-1} and $dn^{\perp}/dT = -3.7 \times 10^{-4}$ °C^{-1} (*12*), showing good agreement with the measured values.

The nylon 1.15:1 fiber produced results of $dn^{\parallel}/dT = -8.3 \times 10^{-5}$ °C^{-1} and $dn^{\perp}/dT = -8.6 \times 10^{-5}$ °C^{-1}. Although no comparative measurement could be found for dn/dT of nylon, the coefficient of thermal expansion of polymers can often be used to estimate their respective dn/dT (*13*). Using this method, the expected dn/dT of nylon 6 would be approximately -1.0×10^{-4} °C^{-1}, confirming that the measured nylon value is likely within an acceptable range of error. The standard deviation in dn/dT for all specimen types is approximately 10% of the measured value. Overall, the results show that the present technique is an acceptable technique for measuring thermo-optic coefficients.

6. Conclusion

This work was done to establish the effectiveness of the wedge interferometer in measuring the refractive index of polymer fibers and to evaluate fiber properties for the purposes of producing polymer-polymer transparent composites. The results of this method of measurement have been shown to match well with the previously established values from the immersion method, as well as interferometric values published in literature. However, there are some limitations to the functionality of the interferometer. Since the fringe shift is a function of the cross-sectional area of material that the light passes through, small fibers produce smaller fringe shifts, and acquiring precise results becomes more difficult. Therefore, it is not recommended to measure fibers smaller than approximately 500 μm^2.

The modifications for measuring dn/dT of polymer fibers in the wedge interferometer have similarly been shown to produce accurate results in the fibers tested. Future work may be useful in fully establishing the effects of birefringence on dn/dT and how it is affected by processing conditions.

Interferometric measurement has been shown to be a valuable tool in defining many of the properties that require consideration when producing fibers for transparent composites. The draw ratio has a potentially strong influence on birefringence, with small changes in the drawing capable of producing large birefringent effects. However, this effect is predicated on the initial conditions of the fiber, and more study is needed on how other variables in processing can affect polymer chain alignment.

Future work on polymer fiber optical characterization will be heavily dependent on the optical properties of the composites produced from these fibers. Links between the fiber properties discussed above and the properties of the resultant composites have yet to be fully established, although related work explores this in more depth. Additionally, a wider range of material and processing variables should be explored in order to gain a more complete understanding of the production possibilities of transparent polymer ribbon fibers.

7. References

1. O'Brien, D. J.; Chin, W. K; Long, L. R.; Wetzel, E. D. *Polymer Matrix, Polymer Ribbon-Reinforced Transparent Composite Materials*; ARL-TR-6201; U.S. Army Research Laboratory: Aberdeen Proving Ground, MD, 2012.

2. Wiley, R. H.; Hobson, P. H. Determination of Refractive Index of Polymers. *Analytical Chemistry* **1948**, *20* (6), 520–523.

3. Liu, Y. S. Direct Measurement of the Refractive Indices for a Small Numerical Aperture Cladded Fiber: A Simple Method. *Applied Optics* **1974**, *13* (6), 1255.

4. Kang, S.; Day, D. E; Stoffer, J. O. Measurement of the Refractive Index of Glass Fibers by the Christiansen-Shelyubskii Method. *J. of Non-Crystalline Solids* **1997**, *220*, 299–308.

5. El-Diasty, F. Characterization of Optical Fibers by Two- and Multiple-Beam Interferometry. *Optics and Lasers in Engineerin*g **2008**, *46*, 291–305.

6. O'Brien, D. J.; Parquette, B.; Hoey, M.; Perry, J. *Development and Optical Characterization of Transparent PP Ribbon-Polymer Composites*; in press; U.S. Army Research Laboratory: Aberdeen Proving Ground, MD, 2013.

7. El-Hennawi, H. A.; El-Diasty, F.; Meshrif, O. Interferometric Determination of the Refractive Index of Optical Fiber Cladding and an Examination of its Homogeneity. *J. of Applied Physics* **1987**, *62*, 4931.

8. Technical Product Guide. AGY, 2009. http://www.agy.com/technical_info/graphics _PDFs/AGY_techguide_17.pdf (accessed 24 August 2013).

9. Hamza, A. A; Fouda, I. M.; El-Farhaty, K. A. Stress Birefringence in Polypropylene Fibres. *Polymer Testing* **1987**, *7*, 329–343.

10. Hamza, A. A.; Fouda, I. M.; El-Farahaty, K. A.; Seisa, E. A. Opto-Mechanical Properties of Fibres 1: Optical Anisotropy in Stretched Nylon 6 Fibres. *Polymer Testing* **1991**, *10*, 82–90.

11. Toyoda, T.; Yabe, M. The Temperature Dependence of the Refractive Indices of Fused Silica and Crystal Quartz. *J. Phys. D: Appl. Phys.* **1983**, *16*, L97–L100.

12. Hamza, A. A.; Sokkar, T. Z. N.; El-Farahaty, K. A.; El-Dessouky, H. M. Influence of Temperature on the Optical and Structural Properties Along the Diameter of: I. Polymer Fibres. *J. Phys.: Condens. Matter* **1999**, *11*, 5331–5341.

13. Zhang, Z.; Zhao, P.; Lin, P.; Sun F. Thermo-Optic Coefficients of Polymers for Optical Waveguide Applications. *Polymer* **2006**, *47*, 4893–4896.

NO. OF
COPIES ORGANIZATION

1 (PDF) DEFENSE TECHNICAL INFORMATION CTR DTIC OCA

1 (PDF) DIRECTOR US ARMY RESEARCH LAB IMAL HRA

1 (PDF) DIRECTOR US ARMY RESEARCH LAB RDRL CIO LL

1 (PDF) GOVT PRINTG OFC A MALHOTRA

ABERDEEN PROVING GROUND

1 (PDF) DIR USARL RDRL WMM A B PARQUETTE